

L-Probe Transmitarrays for X-Band Mobile Communications

Wai-Hau Ng, Kim-Yee Lee, and Eng-Hock Lim*

Abstract—Two novel wire transmitarrays, which are designed using a pair of co-joined L-shaped probes, have been developed for X-band mobile communications. By adjusting the orientation of the L probes, the polarization of the transmitting wave can be easily made either vertical or horizontal. Floquet method has been used for characterizing the transmission responses, and both transmitarray unit cells are found to have achieved a phase range of greater than 380° and a linear phase sensitivity of $44.5^\circ/\text{mm}$. Wide -1 dB gain bandwidth larger than 10% is achievable in both the vertically and horizontally polarized full-fledged transmitarrays, with radiation efficiency of $\sim 90\%$. The proposed transmitarrays have low radar cross section, which can be used for military applications.

1. INTRODUCTION

Transmitarray consists of an array of planar radiating elements fed by a single source. It combines the features of the conventional lens and phase array. The working principle of the transmitarray is akin to lens and it has many advantages such as low profile, light weight, and easy to manufacture. Unlike reflectarray, the radiating elements of the transmitarray are not blocked by its feeding source. Multilayer frequency selective surface (M-FSS) approach is one of the most applied techniques for designing the transmitarray elements. The M-FSS approach requires the use of multiple identical dielectric/air gap layers, stacking on top of each other, for generating sufficient transmission phase range. It was reported in [1] that a single-layer transmitarray element can usually generate phase range of up to 90° . Unit elements such as double square rings [2], spiral dipole [3] and square slot loaded with stubs [4] are the resonators which have been utilized for designing transmitarrays. By sandwiching a PBG element between two annular ring slots [5], such multilayered structure was found to be able to provide a phase range of 360° by involving only two thin dielectric layers. Nonetheless, a mere -1 dB gain bandwidth of 5.7% was achieved in this case.

Dual-polarization antenna arrays are always demanded by military communications as they are not only able to generate high gain, but they can also provide different polarizations for a higher data transfer rate. With the use of the aperture-coupled patches, recently, a dual-polarized transmitarray [6, 7] was successfully designed owing to the good polarization isolation between its coupling slots. Later in [8], rectangular ring slot element was employed for designing a transmitarray which is capable of generating radiation patterns with all types of polarizations. It has been demonstrated [9] that the twisted complementary dual-split ring resonator can also be used for designing a linear polarizer. In this case, the antenna array can function as a reflectarray at low frequency for producing vertically polarized radiation and a transmitarray at high frequency for generating horizontally polarized radiation. At the intermediate frequencies, it can radiate in both directions with different polarizations.

In 1995, the L-shaped wire was found to be useable as an efficient probe for exciting the C-figured loop antennas [10]. Later, it was discovered in [11] that the bandwidth of a microstrip antenna can be

Received 19 March 2017, Accepted 26 May 2017, Scheduled 3 June 2017

* Corresponding author: Eng-Hock Lim (limeh@utar.edu.my).

The authors are with the Department of Electrical and Electronic Engineering, Universiti Tunku Abdul Rahman, Kajang, Selangor, Malaysia.

broadened up to 35% by electromagnetically coupling the energy from an L-shaped probe to the patch. Since then, the L-shaped probe was widely used as proximity excitation source for many antennas such as the dielectric resonator antennas [12], the orthogonally slit cut annular ring microstrip antenna [13], and the E-shaped patch antenna [14]. Due to its advantages such as light weight, low profile, and ease of tuning, the L-shaped probe has also been used for constructing antenna array [15, 16]. Lately, circularly polarized wave with high axial ratio bandwidth is found achievable when the L-shaped probe is incorporated with a waveguide [17, 18] for designing the CP antenna.

For the first time, two L-shaped probes are co-joined for designing two broadband transmitarrays that can transmit with different polarizations for mobile communications in military. By changing the orientation of the L-shaped probes, the transmitting wave can be easily directed into either the horizontal or vertical direction. Unlike the multilayer transmitarrays, the performances of the proposed transmitarrays are not affected by misalignment error. The configurations of the proposed transmitarray elements are first presented in Section 2, where the elements are simulated using a Floquet cell for extracting their transmission properties. Then, parametric analysis is conducted in Section 3. In Section 4, the configurations of the full transmitarrays are elucidated. The two proposed transmitarrays are simulated and experimentally verified, with the measurement setup explained in Section 5. The array performances are demonstrated in Section 6. Finally, the RCS of the proposed element is analyzed in Section 7.

2. TRANSMITARRAY UNIT ELEMENTS

In this section, the configurations of the proposed transmitarray elements are studied. They are designed to generate vertically (y -) and horizontally (x -) polarized waves, as shown in Figures 1 and 2, respectively. The unit element in Figure 1 is described first. Referring to Figure 1(a), the unit element is composed of an FR4 substrate with thickness of $t = 1.7$ mm, dissipation factor of $\tan \delta = 0.025$, and dielectric constant of $\epsilon_r = 4.3$, along with two co-joined conductive probes. The substrate is the structural support for the L probes. In the design, the two probes with a diameter of $d = 1$ mm, which are penetrating through the FR4, are aligned in parallel but separated by a gap of $G_x = 5$ mm. At the height of $h = 10$ mm from the ground plate, the probes on both sides of the substrate are bent 90° into the y -direction. The probes are placed at 4 mm away from the edge of the substrate. Part of the copper, with diameter of $s = 3$ mm, is etched away around the probes for isolation. Two holes ($d = 1$ mm) are then drilled through the substrate for accommodating the probes, and non-conductive adhesive is applied around the probes for holding them. To generate phase change, with reference to Figure 1, the horizontal length l_1 of the long probes on the two sides is varied from 16 to 27.4 mm. The short probe is always shorter than the long probe by $x = 8$ mm, which is optimized by simulation. In simulation, the unit element is placed in an $L \times L$ (31×31 mm²) Floquet cell as illustrated in Figure 1(b). The unit cell is set to have periodic boundaries. Two wave ports, assigned as Port 1 and Port 2, are set

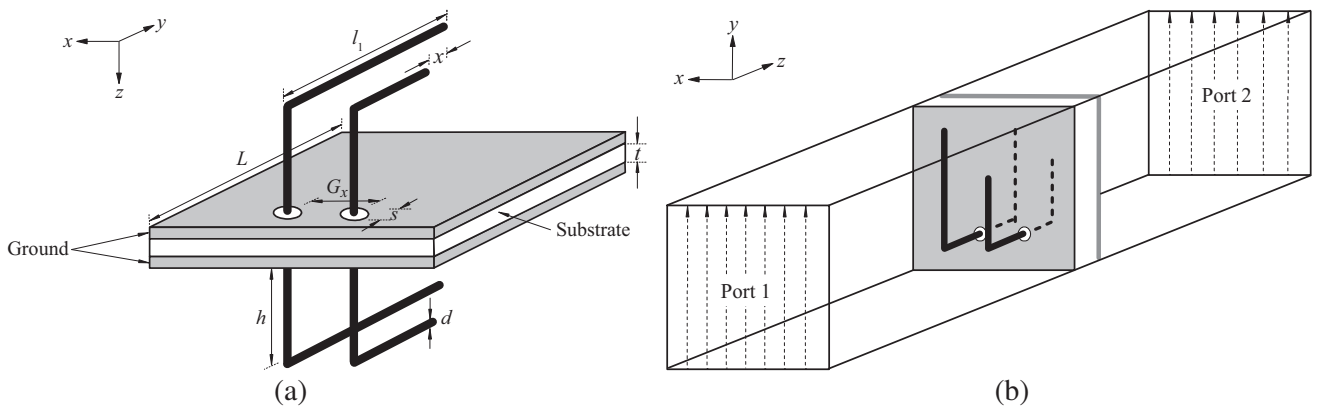


Figure 1. (a) Perspective view, (b) Floquet periodic boundary conditions of the vertically polarized unit cell.

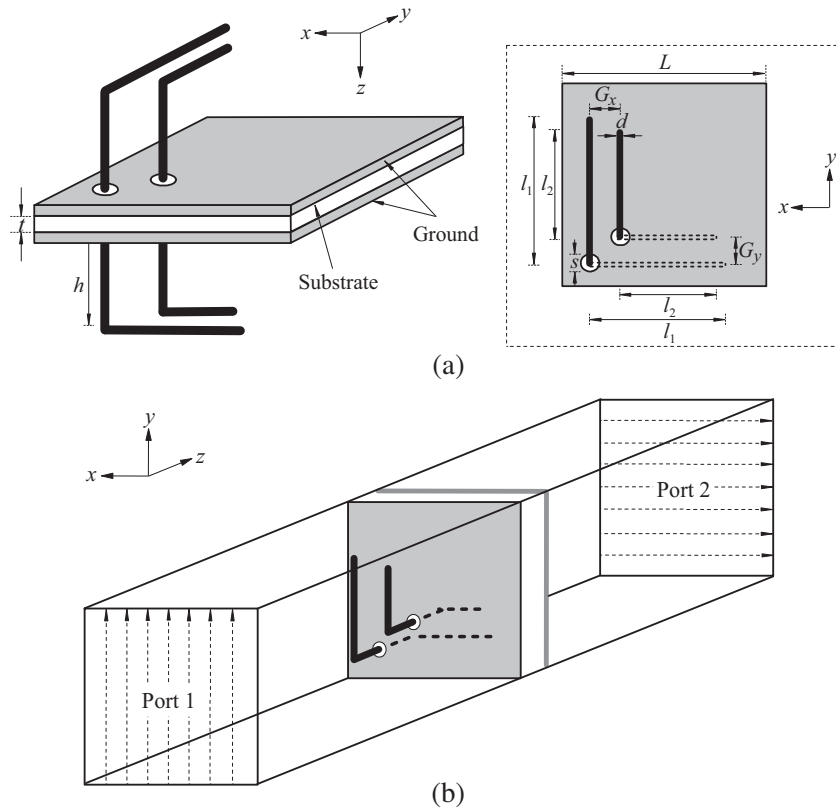


Figure 2. (a) Perspective view, (b) Floquet periodic boundary conditions of the horizontally polarized unit cell.

as the transmitting and receiving ports, respectively, at a distance of 152 mm away from the horizontal parts of the probes. The distance can be of any value as the reference planes are de-embedded flushing with the horizontal probes. A y -polarized plane wave, with a normal incident angle of $\varphi = 0^\circ$, $\theta = 0^\circ$, is launched from Port 1.

By changing the orientation of the horizontal probes, as shown in Figure 2, the unit cell can be made to generate horizontally polarized (x -polarized) wave. This is done by, first, relocating the long probe to a location 4 mm away from the left bottom edge of the substrate while placing the short probe at a distance of $G_x = G_y = 5$ mm away from the long probe. Next, the probes on the transmitting side of unit element are bent 90° pointing to the x -direction. The probe length (l_2) is always shorter than l_1 by $x = 7$ mm ($x = l_1 - l_2$), as shown in Figure 2(a). Again, the two probes on both sides of the substrate are varied simultaneously from $l_1 = 17$ to 27.4 mm to generate transmission phase shift. Other parameters are kept the same as those in Figure 1(a). To enable propagation of the x -polarized wave in the transmitting side of the Floquet cell, the waveport polarization at Port 2 is set to be in the x -direction, as shown in Figure 2(b). Figure 3 shows the transmission magnitudes ($|S_{21}|$) and transmission phases ($\angle S_{21}$) of the transmitarray elements at the center frequency of 7.8 GHz and 7.4 GHz, as described in Figures 1 and 2, respectively. For transmission magnitude of higher than -3 dB, the vertically polarized element is able to produce a maximum phase range of 388° ; whereas the horizontally polarized element is generating 382.89° . Both curves are found to have linear phase response with an average phase sensitivity of $44.5^\circ/\text{mm}$ across the entire range of l_1 , which is not easily achievable by the conventional microstrip structures such as the slotted patch [19] and the Malta crosses with vias [20]. The electric field distributions around the long ($l_1 = 20$ mm) and short ($l_2 = 12$ mm) probes for the vertically polarized unit element are depicted in Figures 4(a) and (b), respectively. Three standing waves (1.5λ) are formed on the long probe while two standing waves (1λ) are found on the short probe, corresponding fairly well with their respective physical lengths of 1.6λ (61.7 mm) and

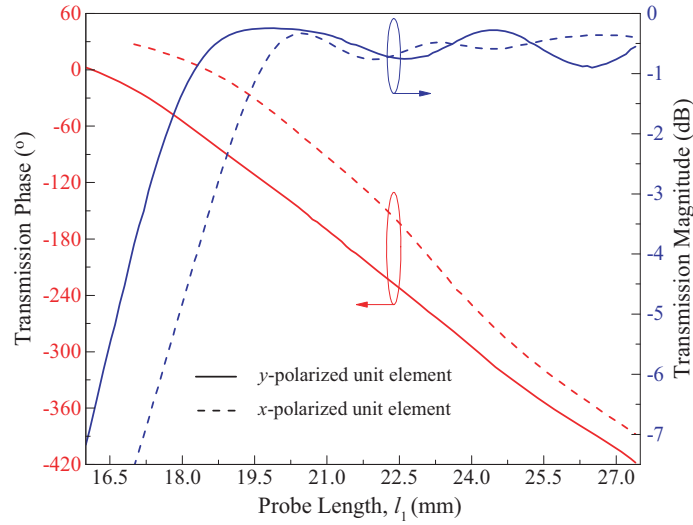


Figure 3. Transmission magnitudes and transmission phases of the transmitarray elements.

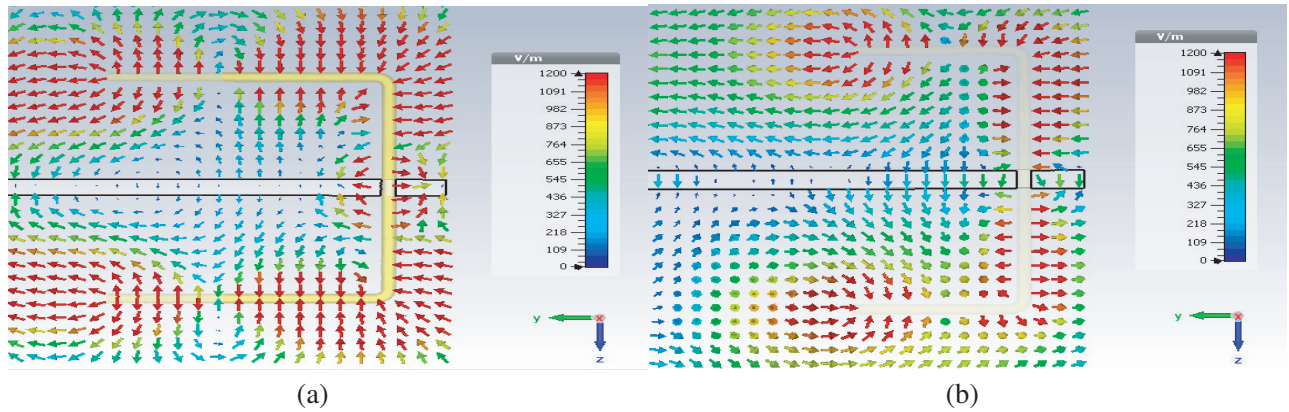


Figure 4. Electric field distributions (side view) around the (a) long probe, (b) short probe at the frequency of 7.8 GHz with $l_1 = 20$ mm for the vertically polarized unit element.

1.19λ (45.7 mm). Broad phase range is achieved by combining the resonances of the L-probes at the two different lengths (1.5λ and 1λ). This technique enables the resonant modes of the multiple L-probes to be combined in a unique way for broadening the phase range of the transmitarray. A similar phenomenon is found on the field distributions of the horizontally polarized element, and the discussion is omitted here.

3. PARAMETRIC ANALYSIS

Parametric analysis has been performed on some of the crucial design parameters in order to study their effects on the performances of the unit elements and full arrays. The vertically polarized transmitarray is analyzed first. To begin, the length difference (x) between the long and the short probes is varied from 0 mm to 9 mm and the element response is shown in Figure 5. Poor transmission of lower than -5.5 dB is observed across all probe lengths when the two probes are made equal in length. It is also observed that the changing rate of the transmission phase curve becomes slower when the length difference between the long and the short probes increases. Figure 6 illustrates the simulated radiation patterns of the vertically polarized transmitarray for different length differences between the long and the short probes. A low boresight ($\theta = 0^\circ$) antenna gain of ~ 19 dBi is obtained for the case of $x = 6$ mm.

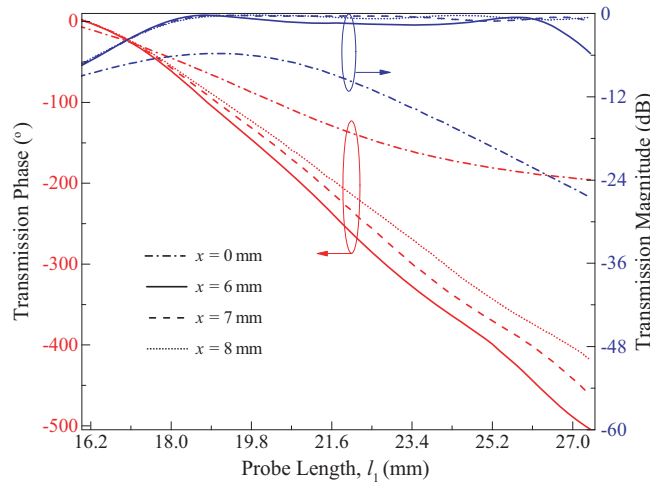


Figure 5. Effects of the length difference (x) between the long and the short probes on the transmission magnitude and transmission phase of the vertically polarized transmitarray unit element.

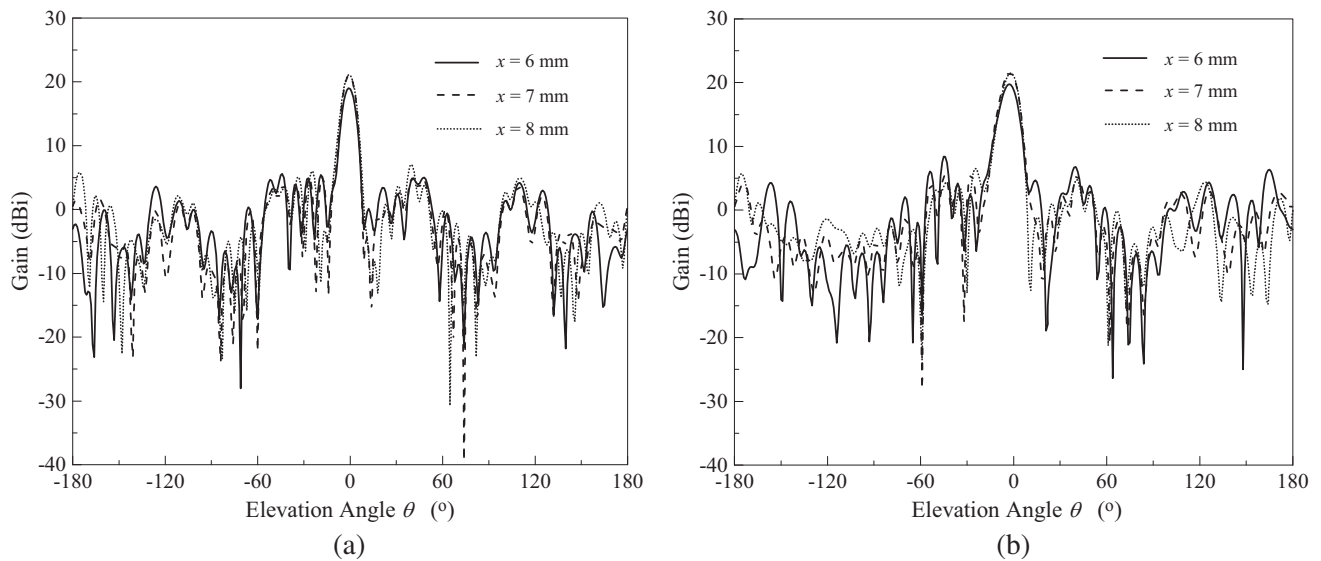


Figure 6. Radiation patterns of the proposed vertically polarized transmitarray for different length differences (x) between the long and the short probes. (a) E - and (b) H -planes.

Effects of the probe diameter (d) are now studied and the simulated results are shown in Figure 7. Poorer transmission is inspected when a thicker probe is deployed. This results in a smaller transmission phase range usable for designing a full array. Change in probe diameter, however, does not affect the linearity of the transmission phase curve. The radiation performances of the full-fledged transmitarray for different probe diameters are shown in Figure 8. For the probe diameter of 0.5 mm, 1 mm, and 1.5 mm, a peak antenna gain of 20 dBi, 21.05 dBi, and 18.22 dBi is achieved, respectively. For the case of $d = 1.5$ mm, a significantly high backlobe level of ~ 10 dBi is also observed, which results in a low front-to-back ratio of 8.22 dBi.

Next, the possible sources of errors in the prototype fabrication are analyzed, and their effects on the transmission characteristics are studied. Errors such as the shortage or extension of the probe height (h), and the mistilt of the probe angle (α), will be discussed thoroughly here. The effect of the probe height (h) is discussed first. With reference to Figure 9, it can be observed that the linearity of the transmission phase curve does not vary much when the probe is shortened ($h = 8$ mm) or lengthened

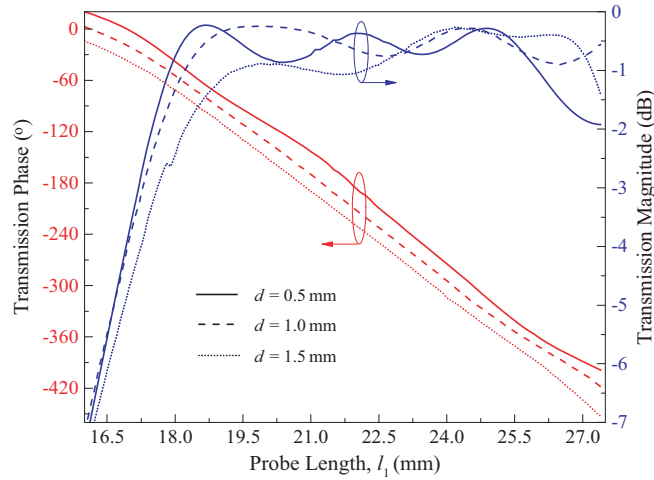


Figure 7. Effects of the probe diameter (d) on the transmission magnitude and transmission phase of the vertically polarized transmitarray unit element.

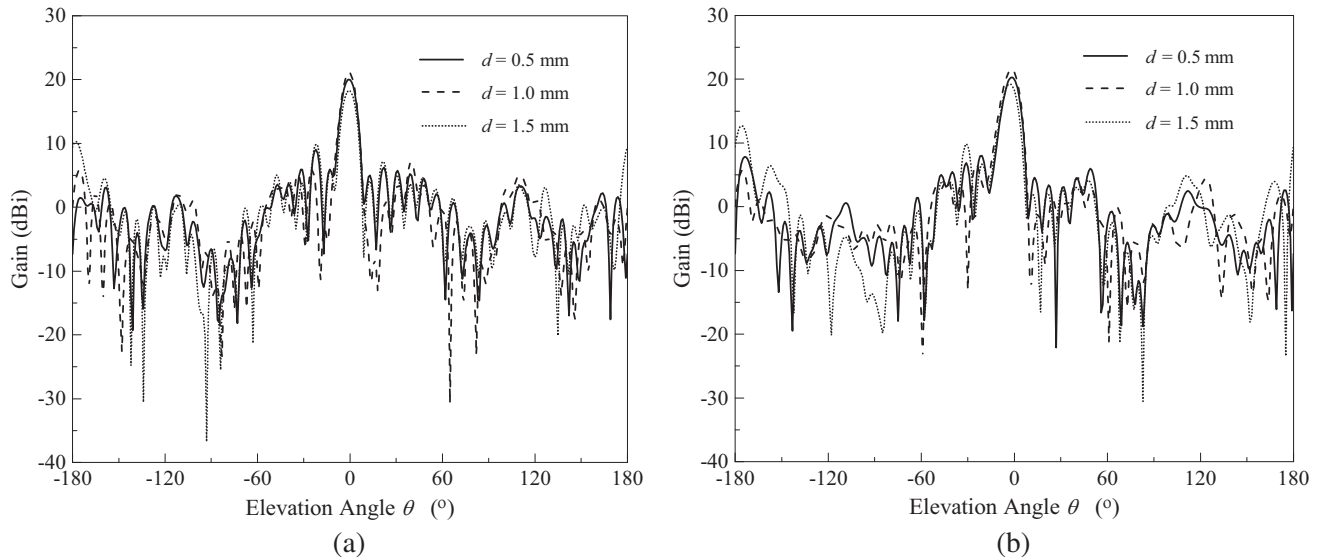


Figure 8. Radiation patterns of the proposed vertically polarized transmitarray for different probe diameters (d). (a) E - and (b) H -planes.

($h = 12$ mm) from the original height ($h = 10$ mm). For all the probe heights, a phase range of more than 360° is achievable with the transmission magnitude maintained well above -3 dB. The effect of the tilt angle (α) of the L-probes is then analyzed. Figures 10(a) and (b) show the horizontal parts of the probes on both sides of the substrate which are tilted in the z - (α_1) and x - (α_2) directions, respectively. For both cases, it is noted that the transmission performances are maintaining almost the same if the error can be kept below 3° for all tilt angles.

The design parameters of the horizontally polarized transmitarray are now studied. The properties of the separation distance between the long and the short probes in the y -direction (G_y) are first analyzed. From the unit element simulation, as can be seen in Figure 11, adjusting G_y from 3 mm to 7 mm does not affect the gradient of transmission phase curve much. Transmission phase range of $\sim 382^\circ$ is obtained for G_y of 3 mm, 5 mm, and 7 mm. In the full-fledged transmitarray, varying the separation distance between the long and the short probes in the y -direction would, however, affect

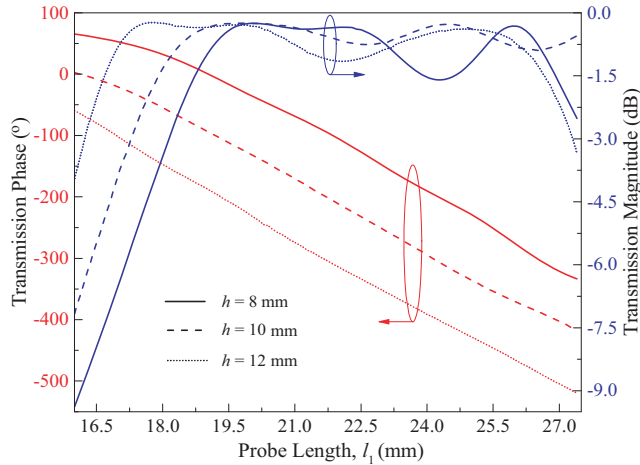


Figure 9. Effects of the probe height (h) on the transmission magnitude and transmission phase of the vertically polarized transmitarray unit element.

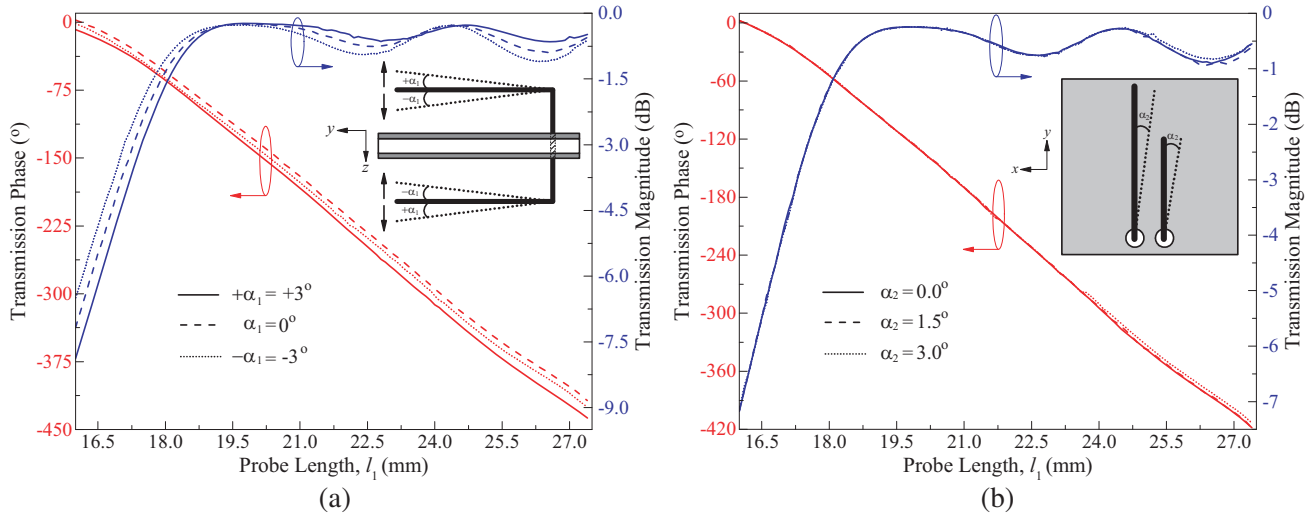


Figure 10. Effects of the tilt angle (α) of the L-probe in the (a) z - and (b) x -directions on the transmission magnitude and transmission phase of the vertically polarized transmitarray unit element.

the radiation performances of the transmitarray. It is observed from Figure 12 that the transmitarrays which are designed with G_y of 3 mm or 7 mm have much higher backlobe level than the one designed with G_y of 5 mm. Similar trends are found in the transmission magnitude and phase responses as well as the radiation patterns when the separation distance between the long and the short probes is varied from 3 mm to 7 mm in the x -direction (G_x).

The unit cell size (L) and element spacing of the full-fledged transmitarray are then studied. Figure 13 shows the transmission magnitude and phase responses of the transmitarray element when the cell size is varied from 0.765λ to 0.814λ at 7.4 GHz. As expected, broader phase range can be achieved for a larger cell size as the probe length can be further lengthened. With reference to the figure, unit cell sizes of 0.765λ , 0.789λ , and 0.814λ have generated phase ranges of 382.89° , 428.92° , and 477.04° , respectively. Varying the cell size does not affect the gradient of the phase curve much. Figure 14 illustrates the radiation patterns of the transmitarray for different element spacings. It is observed that the transmitarray with an element spacing of 0.765λ is able to achieve a higher front-to-back ratio than those for 0.789λ and 0.814λ .

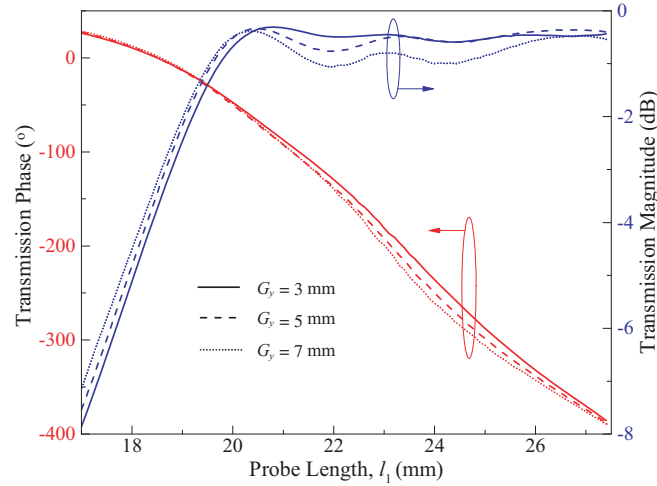


Figure 11. Effects of the separation distance between the long and the short probes in the y -direction (G_y) on the transmission magnitude and transmission phase of the horizontally polarized transmitarray unit element.

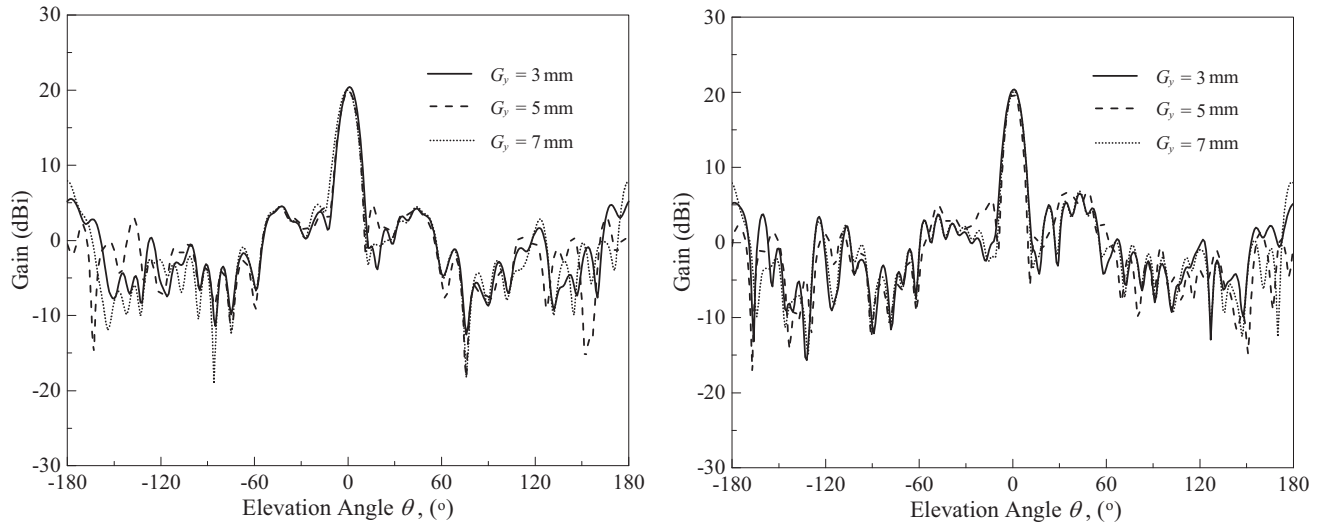


Figure 12. Simulated radiation patterns of the proposed horizontally polarized transmitarray for different probe separations in the y -direction (G_y). (a) E - and (b) H -planes.

4. FULL TRANSMITARRAYS

With the use of the transmission phase curves in Figure 3, the unit elements are designed into the full-fledged transmitarrays shown in Figure 15. By properly compensating the propagation path length for the N th element (P_N) with respect to the reference (P_0), a cophasal re-radiated wave can be generated in the boresight direction. The design parameters of the two transmitarrays are described now. It can be seen from Figure 15 that the transmitarrays are assembled from 81 elements (9×9). For the vertically and horizontally polarized transmitarrays, the element sizes are set to be $L = 0.806\lambda = 31$ mm and $L = 0.765\lambda = 31$ mm, respectively. A linearly polarized pyramidal horn (5.85–8.2 GHz) is used to excite the two transmitarray elements where the horn is placed at the focal length of $f = 223.2$ mm from the middle point. In this case, the edge tapering for the two transmitarrays is $38.16^\circ \cdot \cos^q \theta$ has also been used for modelling the radiation patterns of the feed horn. The horn has antenna gains of 10.9 dBi and 11.3 dBi, and q values of 6.2 and 6.44 at the operating frequencies of 7.4 GHz and 7.8 GHz,

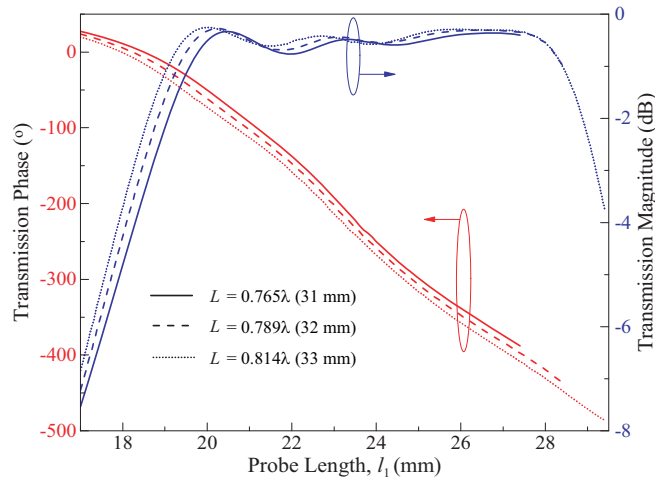


Figure 13. Effects of the unit element dimension (L) on the transmission magnitude and transmission phase of the horizontally polarized transmitarray unit element.

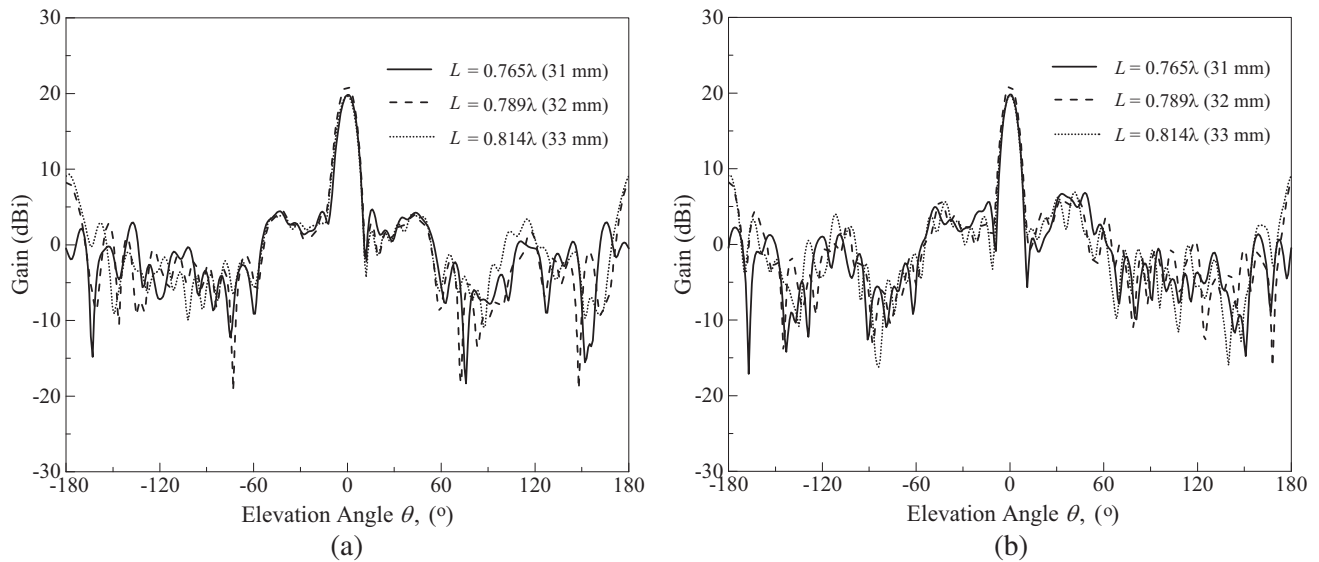


Figure 14. Simulated radiation patterns of the proposed horizontally polarized transmitarray for different separation distances (L). (a) E - and (b) H -planes.

respectively. Figures 16(a)–(d) show the simulated reflection coefficient, radiation patterns, gain versus frequency, and phase center variation versus frequency of the feed horn, respectively. It must be pointed out that the phase center of the horn, depicted in Figure 16(d) is the distance from the center of the horn aperture (Δz). For both, the resulting f/D ratio is 0.8 where $D = 9L = 279$ mm. The prototype of the vertically polarized transmitarray is shown in Figure 17. The top and bottom ground layers are connected by 3M copper tapes so that they are equi-potential.

5. MEASUREMENT SETUP

Figure 18 shows the free space experimental setup for measuring the antenna gains and radiation patterns of the antenna under test (transmitarrays). The antenna under test (AUT), which is the transmitting antenna, is connected to a signal generator (Rohde & Schwarz SMB100A) for generating

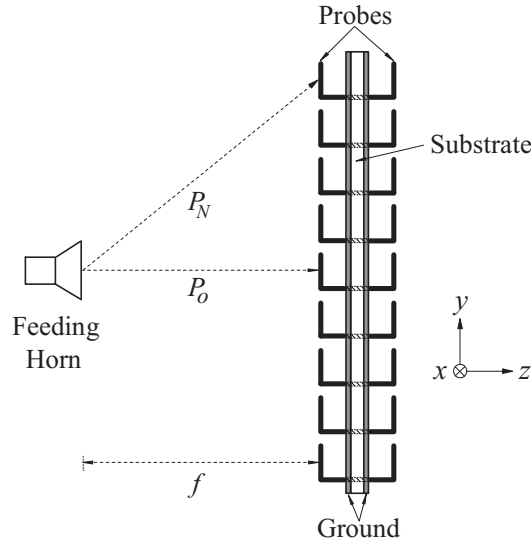
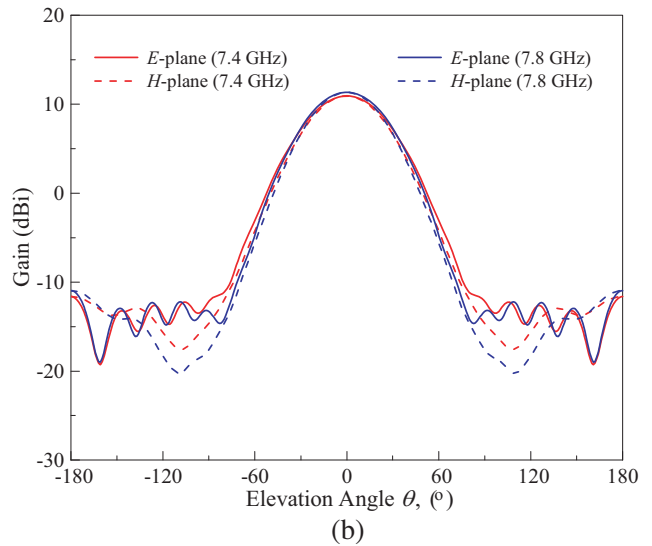
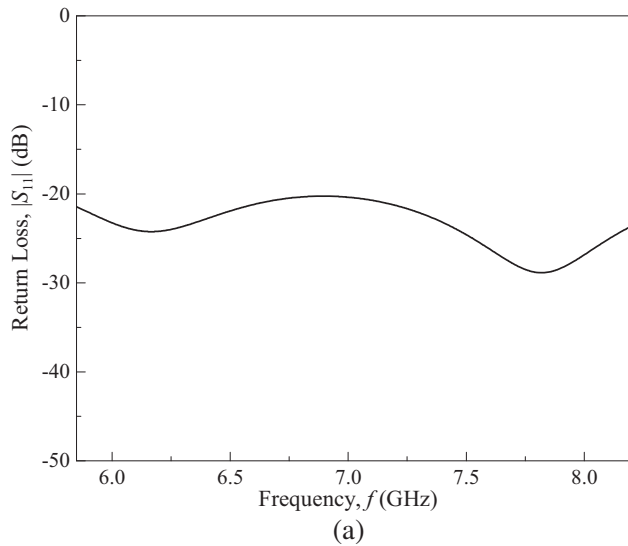


Figure 15. Configuration of the proposed vertically polarized transmitarray.

microwave signal. The signal generator is tuned to the operating frequency of AUT. To capture the received power P_r , a pyramidal horn (ATM PNR137-440-2, 5.85 GHz–8.2 GHz), which is the receiving antenna, is connected to a spectrum analyzer (Advantest U3771). It is placed at a far field distance of $R \geq 2D^2/\lambda$, where D is the diagonal dimension of the AUT. In measurement, a power of $P_t = -10$ dBm is supplied from the signal generator, and the AUT is rotated on a turntable in the θ direction for a full cycle of 360° . For different elevation angles, the received powers are directly read from the spectrum analyzer. The gain of the AUT for each elevation angle is found by applying the Friss transmission formula.

6. RESULTS AND DISCUSSION

Figure 19 shows the measured and simulated radiation patterns of the vertically polarized (y -polarized) transmitarray in the yz -plane (E -plane) and xz -plane (H -plane). At the elevation angle of $\theta = 0^\circ$, it has a measured gain of 21.91 dBi (simulation: 21.05 dBi) at 7.8 GHz, which corresponds to an aperture



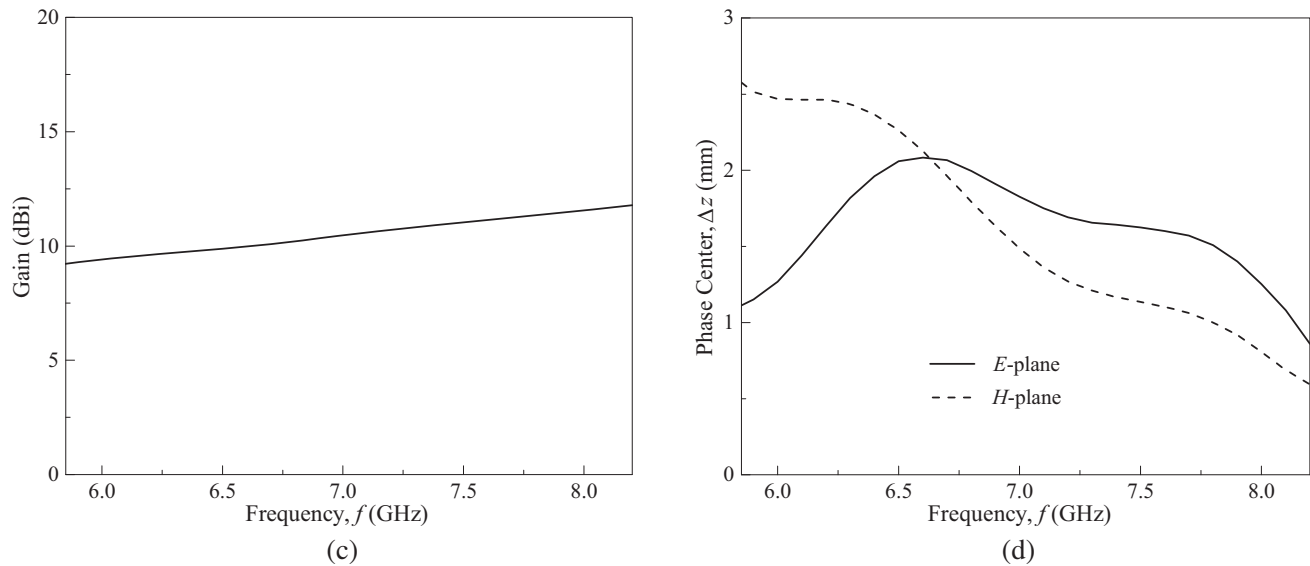


Figure 16. Simulated (a) reflection coefficient, (b) radiation patterns, (c) gain versus frequency, and (d) phase center variation versus frequency of the linearly polarized pyramidal horn (5.85–8.2 GHz).

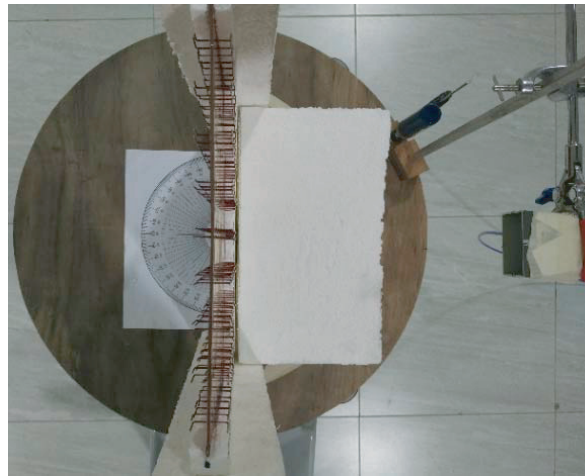


Figure 17. Prototype of the vertically polarized transmitarray.

efficiency of 23.5%. The cross-polarized field is at least 30 dB smaller than its co-polarized counterpart in the boresight direction ($\theta = 0^\circ$). For the horizontally polarized (x -polarized) transmitarray, it is observed from Figure 20 that broadside radiation pattern with a measured peak gain of 19.05 dBi (simulation 19.78 dBi) has been obtained. This corresponds to an aperture efficiency of 13.9% (simulation: 16.4%). It should be pointed out that the xz -plane is the E -plane while the yz -plane is the H -plane in this case. The co-polarized and cross-polarized fields at the elevation angle of $\theta = 0^\circ$ are different by 21.34 dB. The simulated radiation efficiencies of the vertically and horizontally polarized transmitarrays are found to be 92.4% and 89.5%, respectively. The antenna gains of both the proposed transmitarrays are shown in Figure 21. The vertically polarized transmitarray has a measured -1 dB gain bandwidth of 11.62% (simulation: 11.92%), covering 7.3 GHz–8.2 GHz (simulation: 7.1 GHz–8 GHz). And the horizontally polarized transmitarray has a measured -1 dB gain bandwidth of 10.39%, (covering 7.3 GHz–8.1 GHz), being slightly lower than the simulated bandwidth of 12.79% (covering 6.95 GHz to 7.9 GHz).

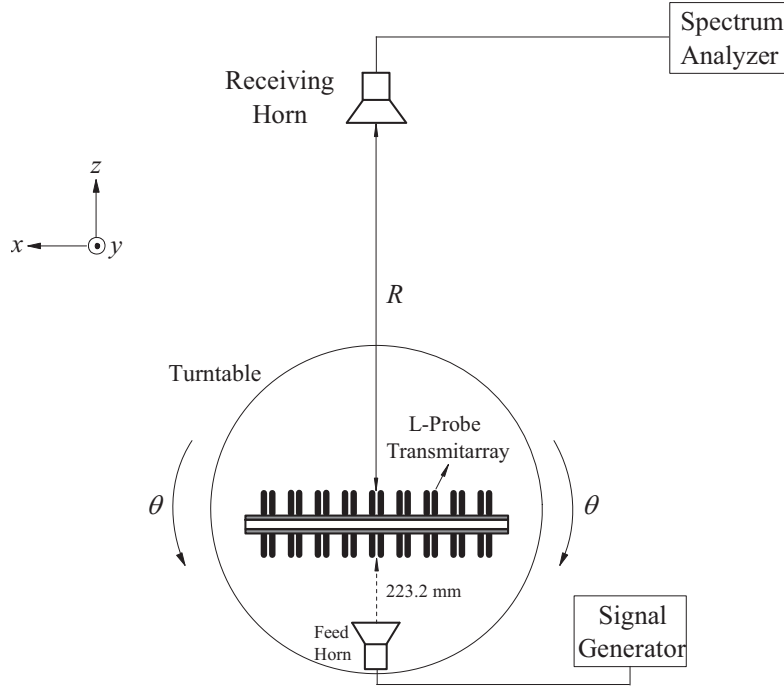


Figure 18. Measurement setup for the transmitarrays.

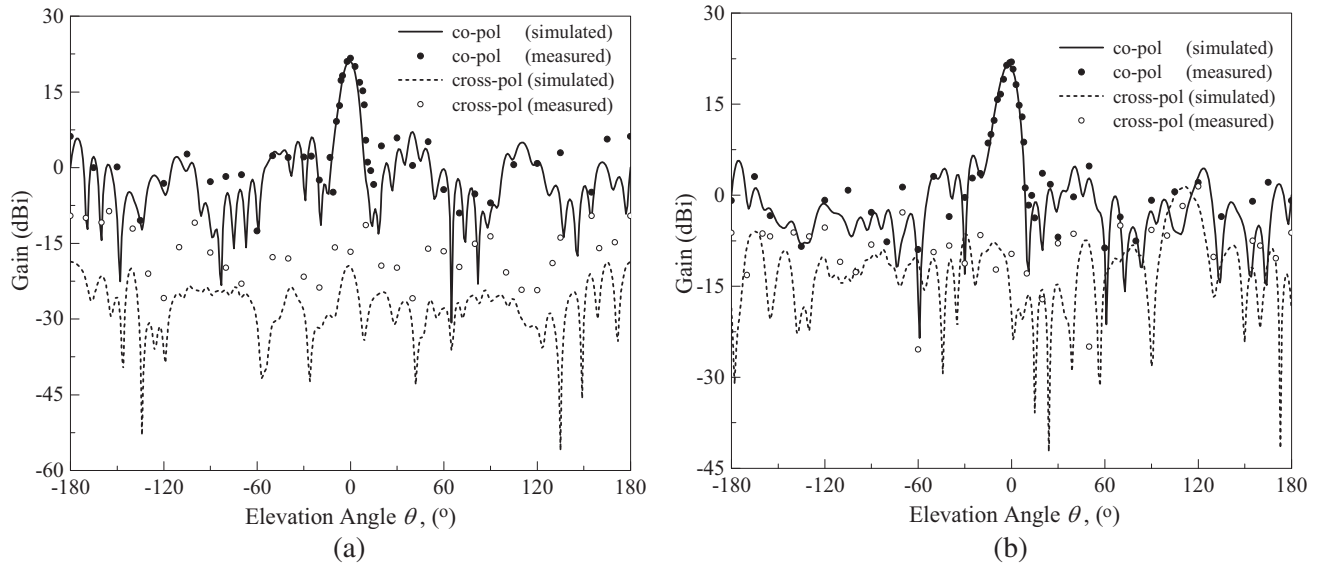


Figure 19. Measured and simulated (a) E - and (b) H -plane radiation patterns of the vertically polarized transmitarray.

The reflection characteristic of the vertically polarized transmitarray is now discussed. Figures 22(a)–(c) illustrate the electric fields of the feed horn, the electric fields of the transmitarray with the feed horn, and the scattered electric fields of the transmitarray obtained by subtracting away the fields of the feed horn, respectively. It can be seen from Figure 22(c) that only a small portion of the incident electric field from the feed horn is reflected by the transmitarray. The spillover of the two transmitarrays is then discussed. By applying the formula in [21], the spillover efficiencies of the vertically and horizontally polarized transmitarrays are approximated to be 89.8% and 89%,

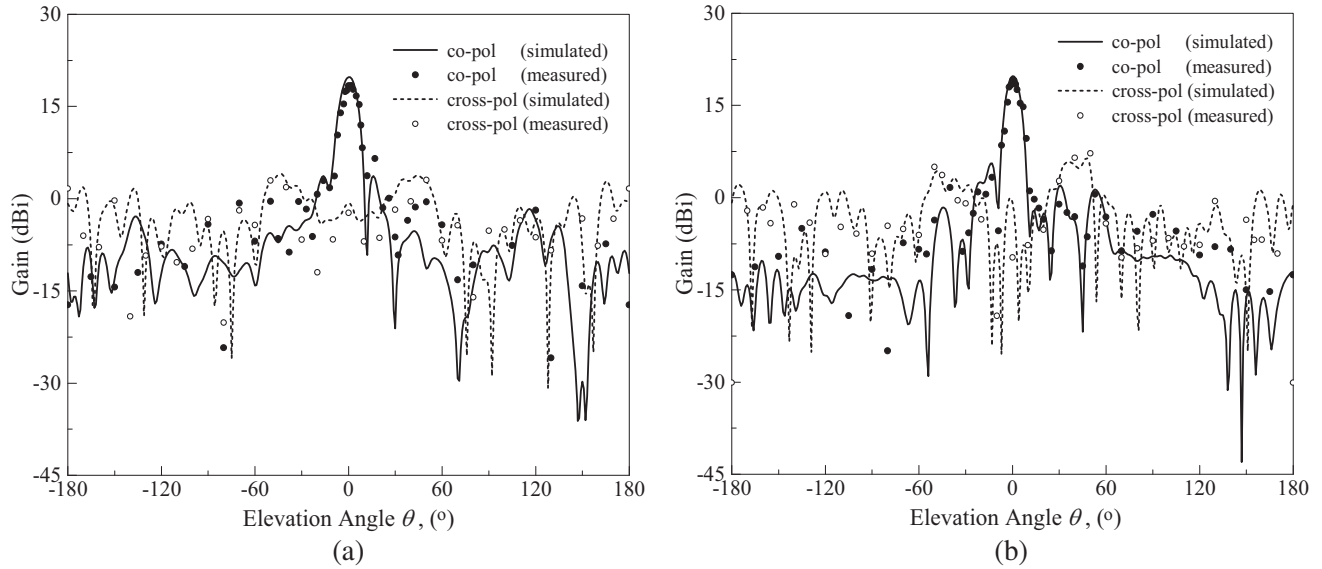


Figure 20. Measured and simulated (a) *E*- and (b) *H*-plane radiation patterns of the horizontally polarized transmitarray.

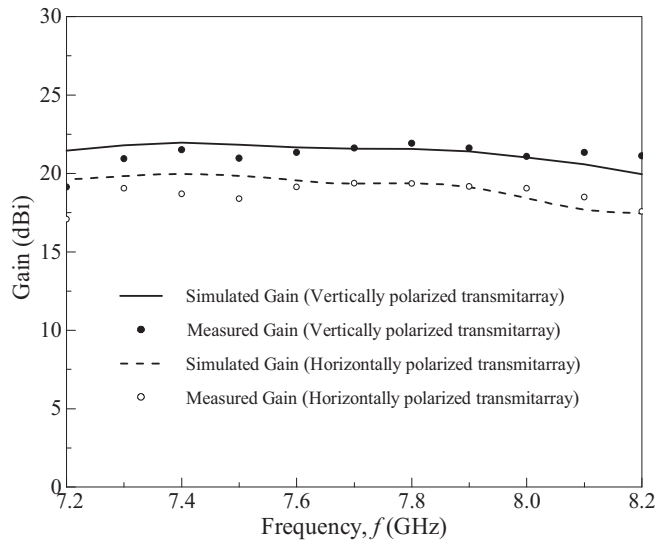


Figure 21. Measured and simulated antenna gains of the vertically and horizontally polarized transmitarrays.

respectively. This shows that only 11% of the radiated power from the feed horn is not intercepted by the transmitarray apertures. To study the effects of the probe manufacturing tolerances on the radiation patterns of the vertically polarized transmitarray, the probe lengths(l_1) of the transmitarray is purposely set to be ± 1 mm different from the original length. Figure 23 shows the simulated radiation patterns of the vertically polarized transmitarray for the cases with and without manufacturing tolerances. It can be concluded that changes of ± 1 mm in the probe length only reduce the boresight gain by ~ 1.3 dBi.

Table 1 compares the performances of the proposed transmitarrays with some of the recently published works. Referring to the table, the conducting layers of the transmitarrays in [8, 22–24] are separated by an air gap which is dependent on the operating frequency. When designed at 7.8 GHz, each of the transmitarrays has a thickness of 21.23 mm, 28.85 mm, 19.73 mm, and 29.35 mm, respectively. It is worth noting that the proposed transmitarrays have about the same structure thickness of those

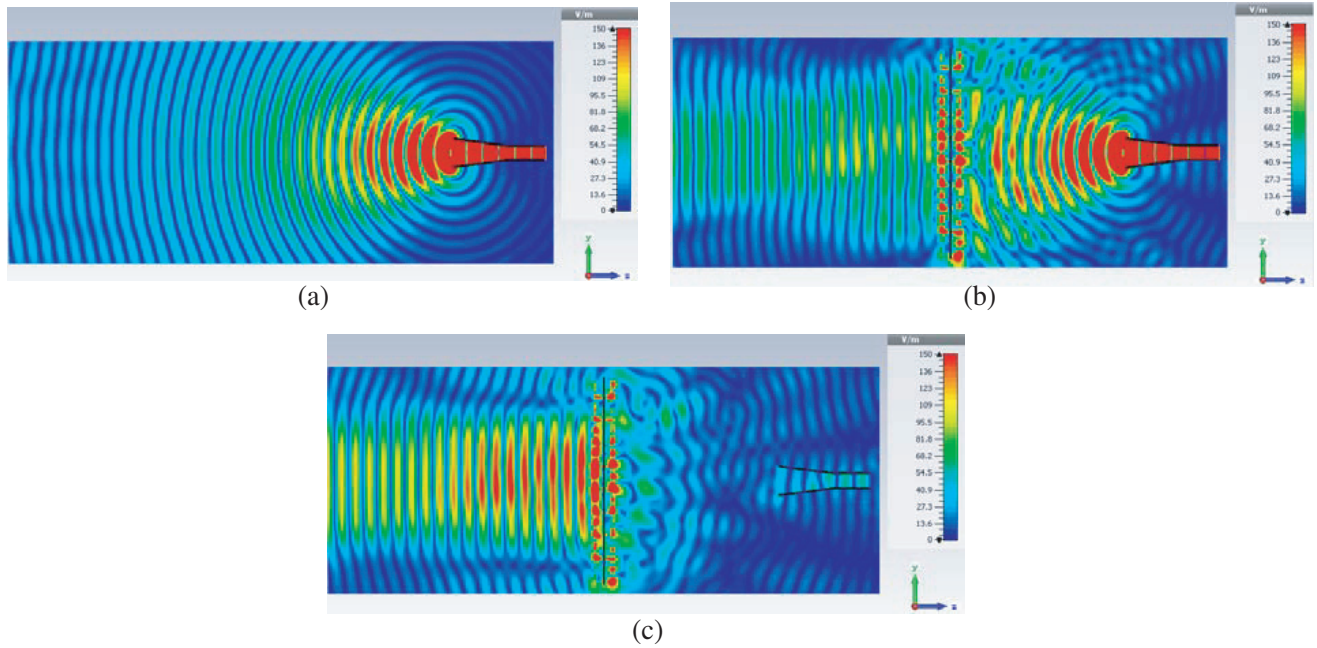


Figure 22. (a) Electric fields of the feed horn. (b) Electric fields for the vertically polarized transmitarray with the feed horn. (c) Scattered electric fields of the transmitarray which is obtained by subtracting away the fields of the feed horn.

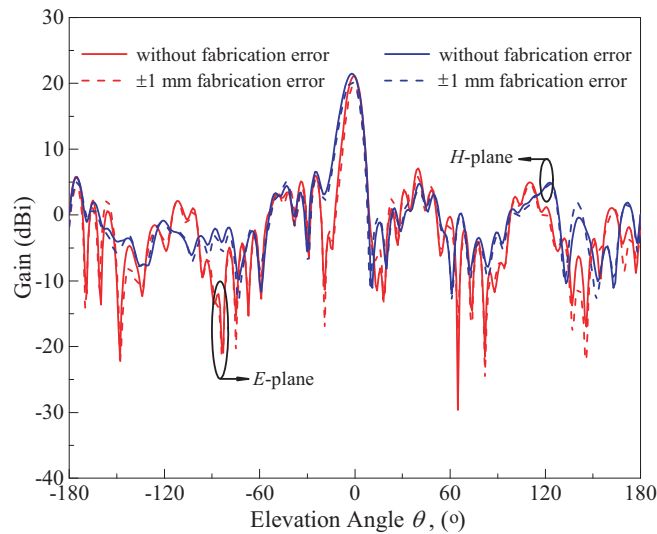


Figure 23. Simulated radiation patterns of the vertically polarized transmitarray with (± 1 mm) and without manufacturing tolerances.

in [8, 22–24], while maintaining a low phase sensitivity. With the same number of elements as those in [8] and [23], and lesser than that in [9], our proposed transmitarrays have managed to achieve higher antenna gain and -1 dB gain bandwidth. The transmitarray in [22] has an antenna gain of 23.76 dBi, but it requires a total of 325 slot elements to achieve an aperture efficiency of only 14.2% and a -1 dB gain bandwidth of only 4.2%, which are lower than the proposed transmitarrays. In [7], the transmitarray has a total thickness of 3.149 mm, which is low in profile. However, the transmitarray element is only able to provide a total phase range of 210° , which is insufficient for designing a very

large-size transmitarray. Besides that, the proposed transmitarrays eliminate the misalignment problem that can occur in a multilayer structure. Both of the proposed transmitarrays have reasonable antenna gains, aperture efficiencies, and -1 dB gain bandwidths. Due to the conductive loss of the L-probes, the proposed transmitarrays are more suitable for low-frequency applications.

Table 1. Comparison of the proposed transmitarrays with the recently published works.

Reference Number	Number of Conducting Layer (s)	Structure Thickness (mm)	Phase Sensitivity ($^{\circ}$ /mm)	Gain (dBi)	Aperture Efficiency (%)	$-1/-3$ dB Gain Bandwidth (%)
Vertically polarized	-	24.7	44.5	21.91	23.5	11.62
Horizontally polarized	-	24.7	44.5	19.05	13.9	10.39
(This work)						
[7]	3	3.149	-	24.9	24.6	20*
[8]	3	30 @ 6 GHz	25	20.1	27	8.3
[9]	3	3	166.7	18.5	28	6.7
[22]	4	19.92 @ 11.3 GHz	144.8	23.76	14.2	4.2
[23]	3	12.5 @ 12.5 GHz	83.6	18.9	20.9	9.6
[24]	4	17 @ 13.5 GHz	70.8	23.8	12.4	-

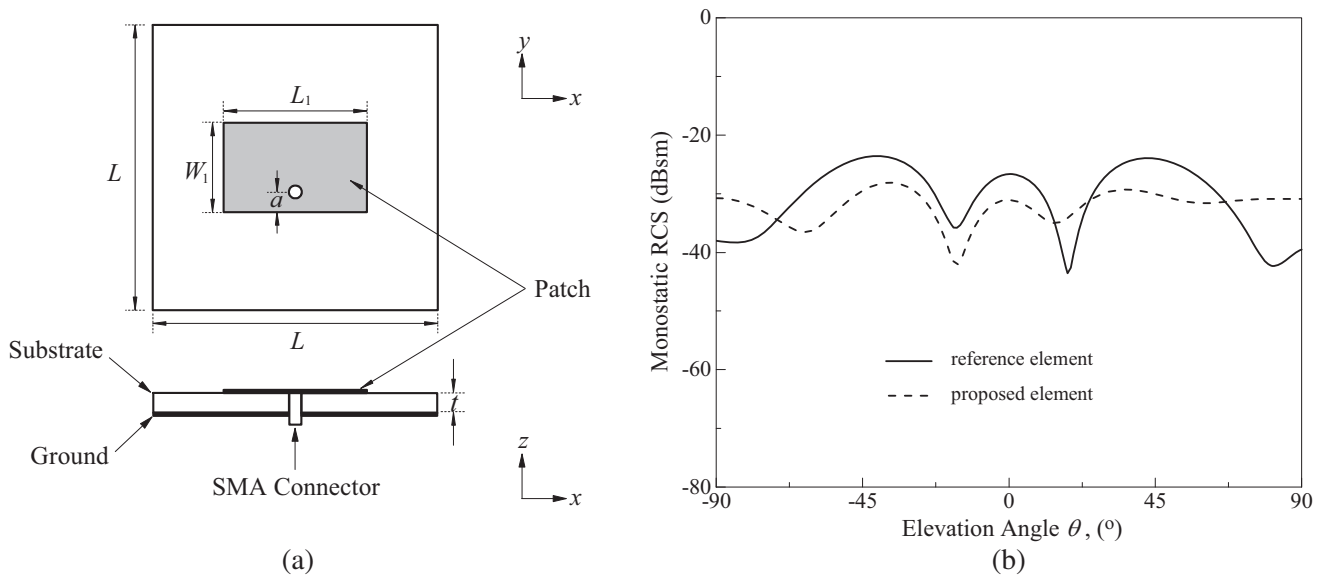


Figure 24. (a) Configuration of the conventional coaxially fed microstrip patch antenna. (b) Comparison between the monostatic RCS of the reference and proposed elements for a y -polarized plane wave.

7. RADAR CROSS SECTION

In this section, the radar cross section (RCS) of the vertically polarized transmitarray element (proposed) with the probe length of $l_1 = 27.4$ mm is compared with that for the conventional coaxially fed microstrip patch antenna (reference) at the operating frequency of 7.8 GHz, as shown in Figure 24(a). The reference antenna has a dimension of $L_1 = 14.78$ mm, and $W_1 = 8.25$ mm and it is printed on an FR4 substrate, which is designed following the cell size and resonant frequency of the unit element. The SMA port is fed at the distance of $a = 2.125$ mm from the edge of the patch. Figure 24(b) shows the monostatic RCS of the reference and proposed elements, impinging by a y -polarized plane wave at different incident angles in the E -plane. It can be clearly observed that the proposed unit element has lower RCS when normally impinged by a plane wave. Also, the proposed unit element has lower RCS in overall for different oblique incident plane waves, making it more advantageous for military applications.

8. CONCLUSION

Two L-shaped probes are co-joined for designing the vertically and horizontally polarized broadband transmitarrays. The unit elements have achieved a linear transmission phase range of greater than 380° with low phase sensitivity of $44.5^\circ/\text{mm}$, and both of the full-fledge transmitarrays have generated a -1 dB gain bandwidth of more than 10%. Parametric analysis has been performed on several crucial geometrical parameters and it is found that the design parameters easily optimized for achieving optimal performances. Since the proposed transmitarrays do not require stacking multiple substrates, misalignment problem can be avoided in the fabrication processes. The proposed transmitarrays can be used for military communications as they have lower RCS than the conventional patch arrays.

REFERENCES

1. Abdelrahman, A. H., A. Z. Elsherbeni, and F. Yang, "Transmission phase limit of multilayer frequency-selective surfaces for transmitarray designs," *IEEE Trans. Antennas Propag.*, Vol. 62, No. 2, 690–697, Feb. 2014.
2. Ryan, C. G. M., M. R. Chaharmir, J. Shaker, J. R. Bray, Y. M. M. Antar, and A. Ittipiboon, "A wideband transmitarray using dual-resonant double square rings," *IEEE Trans. Antennas Propag.*, Vol. 58, No. 5, 1486–1493, May 2010.
3. Abdelrahman, A. H., A. Z. Elsherbeni, and F. Yang, "High-gain and broadband transmitarray antenna using triple-layer spiral dipole elements," *IEEE Antennas Wireless Propag. Lett.*, Vol. 13, 1288–1291, 2014.
4. Rahmati, B. and H. R. Hassani, "High-efficient wideband slot transmitarray antenna," *IEEE Trans. Antennas Propag.*, Vol. 63, No. 11, 5149–5155, Nov. 2015.
5. Rahmati, B. and H. R. Hassani, "Low-profile slot transmitarray antenna," *IEEE Trans. Antennas Propag.*, Vol. 63, No. 1, 174–181, Jan. 2015.
6. Plaza, E. G., G. Leon, S. Lored, and F. Las-Heras, "Dual polarized transmitarray lens," *2014 8th European Conference on Antennas and Propagation*, 2305–2308, 2014.
7. Pham, K., N. T. Nguyen, A. Clemente, L. D. Palma, L. L. Coq, L. Dussopt, and R. Sauleau, "Design of wideband dual linearly polarized transmitarray antennas," *IEEE Trans. Antennas Propag.*, Vol. 64, No. 5, 2022–2026, May 2016.
8. Zhong, X., L. Chen, S. Yan, and X. Shi, "Design of multiple polarization transmitarray antenna using rectangle ring slot elements," *IEEE Antennas Wireless Propag. Lett.*, Vol. 15, 1803–1806, 2016.
9. Xu, H. X., S. Tang, G. M. Wang, T. Cai, W. Huang, Q. He, S. Sun, and L. Zhou, "Multifunctional microstrip array combining a linear polarizer and focusing metasurface," *IEEE Trans. Antennas Propag.*, Vol. 64, No. 8, 3676–3682, Aug. 2016.
10. Nakano, H., H. Yoshida, and Y. Wu, "C-shaped loop antennas," *Electron. Lett.*, Vol. 31, No. 9, 693–694, Apr. 1995.

11. Luk, K. M., C. L. Mak, Y. L. Chow, and K. F. Lee, "Broadband microstrip patch antenna," *Electron. Lett.*, Vol. 34, No. 15, 1442–1443, Jul. 1998.
12. Kishk, A. A., R. Chair, and K. F. Lee, "Broadband dielectric resonator antennas excited by L-shaped probe," *IEEE Trans. Antennas Propag.*, Vol. 54, No. 8, 2182–2189, Aug. 2006.
13. Singh, A. K., R. K. Gangwar, and B. K. Kanaujia, "Bandwidth enhancement of L-probe proximity-fed annular ring microstrip slot antenna," *2013 6th International Conference on Advanced Infocomm Technology*, 195–197, 2013.
14. Zheng, J., G. Hu, X. Hu, and J. Gu, "E-shaped patch antenna using L-probe for 4G communication systems," *Sensors Transducers*, Vol. 182, No. 11, 105–110, Nov. 2014.
15. Wang, H., K. L. Lau, and K. M. Luk, "Design of dual-polarized L-probe patch antenna arrays with high isolation," *IEEE Trans. Antennas Propag.*, Vol. 52, No. 1, 45–52, Jan. 2004.
16. Wang, L., Y. X. Guo, and W. X. Sheng, "Wideband high-gain 60-GHz LTCC L-probe patch antenna array with a soft surface," *IEEE Trans. Antennas Propag.*, Vol. 61, No. 4, 1802–1809, Apr. 2013.
17. Yamauchi, R. and T. Fukusako, "Circularly polarized broadband waveguide antenna using L-shaped probe," *2014 IEEE International Workshop on Electromagnetics*, 237–238, 2014.
18. Yamauchi, R. and T. Fukusako, "Reduction of cross polarization for circularly polarized broadband waveguide antenna," *2015 International Workshop on Electromagnetics*, 1–2, 2015.
19. Liu, G., H. J. Wang, J. S. Jiang, F. Xue, and M. Yi, "A high-efficiency transmitarray antenna using double split ring slot elements," *IEEE Antennas Wireless Propag. Lett.*, Vol. 14, 1415–1418, 2015.
20. An, W., S. Xu, F. Yang, and M. Li, "A double-layer transmitarray antenna using Malta crosses with vias," *IEEE Trans. Antennas Propag.*, Vol. 64, No. 3, 1120–1125, Mar. 2016.
21. Yu, A., F. Yang, A. Z. Elsherbeni, J. Huang, and Y. Rahmat-Samii, "Aperture efficiency analysis of reflectarray antennas," *Microw. Opt. Technol. Lett.*, Vol. 52, 364–372, Feb. 2010.
22. Abdelrahman, A. H., A. Z. Elsherbeni, and F. Yang, "Transmitarray antenna design using cross-slot elements with no dielectric substrate," *IEEE Antennas Wireless Propag. Lett.*, Vol. 13, 177–180, 2014.
23. Yu, J., L. Chen, J. Yang, and X. Shi, "Design of a transmitarray using split diagonal cross elements with limited phase range," *IEEE Antennas Wireless Propag. Lett.*, Vol. 15, 1514–1517, 2016.
24. Abdelrahman, A. H., P. Nayeri, A. Z. Elsherbeni, and F. Yang, "Single-feed quad-beam transmitarray antenna design," *IEEE Trans. Antennas Propag.*, Vol. 64, No. 3, 953–959, Mar. 2016.